Microstructural-informed plasticity with reinforcement learning guided data exploration

Steve WaiChing Sun
Department of Civil Engineering and Engineering Mechanics
Columbia University

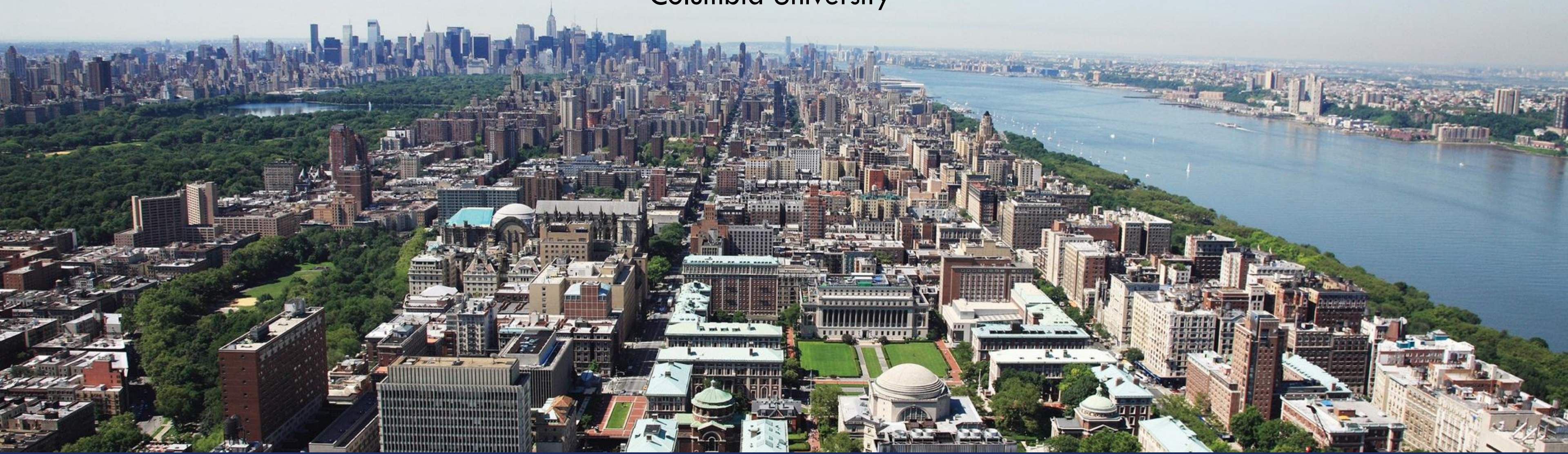

Augmented Intelligence Research Workflow for material modeling

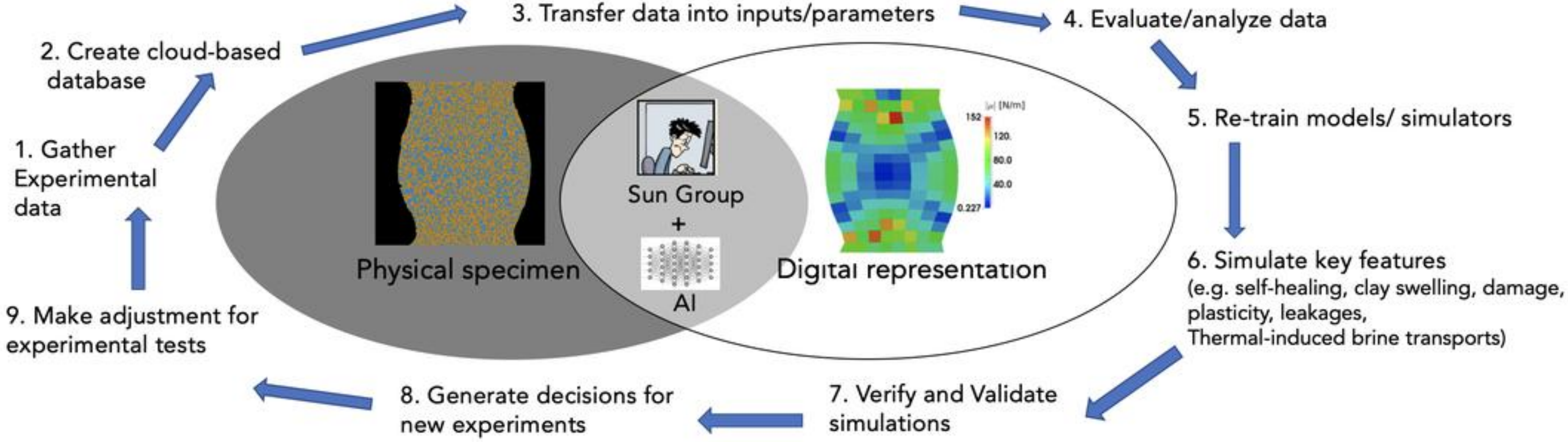

1. How fast can this workflow be?
2. How much improvement for each iteration? And at what cost?
3. How to deal with different data?
4. Which part of the workflow can be automated, which part cannot?

*Highlight 1: Physics-informed **interpretable** material modeling*

The state-of-the-art material models

Von Mises J2 plasticity 1910s

Drucker-Prager 1950s

Critical state soil mechanics 1960s

Sand model with fabric tensor 2004

Dependence on mean effective pressure

Dependence on void ratio

Dependence on fabric tensor

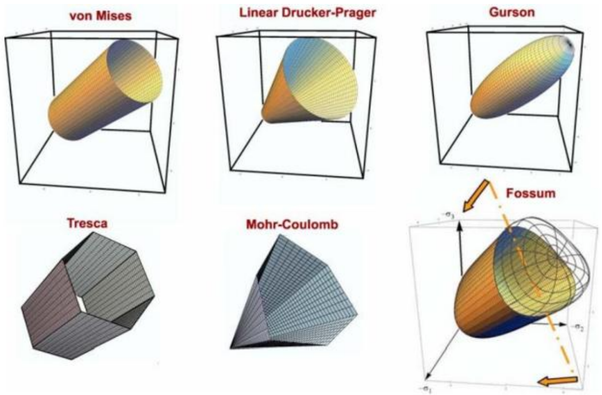

Figure from Rebecca Brannon

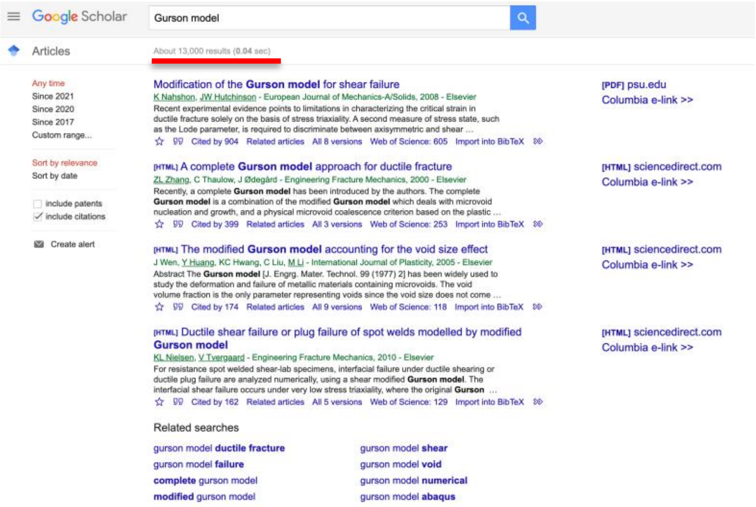

Google Scholar

Gurson model

Articles

About 13,000 results (0.04 sec)

Any time
Since 2021
Since 2020
Since 2017
Custom range...

Sort by relevance
Sort by date

include patents
include citations

Create alert

Modification of the **Gurson model** for shear failure
K Nahshon, JW Hutchinson - European Journal of Mechanics-A/Solids, 2008 - Elsevier
Recent experimental evidence points to limitations in characterizing the critical strain in ductile fracture solely on the basis of stress triaxiality. A second measure of stress state, such as the Lode parameter, is required to discriminate between axisymmetric and shear ...
Cited by 904 Related articles All 8 versions Web of Science: 605 Import into BibTeX
[PDF] psu.edu
Columbia e-link >>

[HTML] A complete **Gurson model** approach for ductile fracture
ZL Zhang, C Thaulow, J Ødegård - Engineering Fracture Mechanics, 2000 - Elsevier
Recently, a complete **Gurson model** has been introduced by the authors. The complete **Gurson model** is a combination of the modified **Gurson model** which deals with microvoid nucleation and growth, and a physical microvoid coalescence criterion based on the plastic ...
Cited by 399 Related articles All 3 versions Web of Science: 253 Import into BibTeX
[HTML] sciencedirect.com
Columbia e-link >>

[HTML] The modified **Gurson model** accounting for the void size effect
J Wen, Y Huang, KC Hwang, C Liu, M Li - International Journal of Plasticity, 2005 - Elsevier
Abstract The **Gurson model** [J. Engrg. Mater. Technol. 99 (1977) 2] has been widely used to study the deformation and failure of metallic materials containing microvoids. The void volume fraction is the only parameter representing voids since the void size does not come ...
Cited by 174 Related articles All 9 versions Web of Science: 118 Import into BibTeX
[HTML] sciencedirect.com
Columbia e-link >>

[HTML] Ductile shear failure or plug failure of spot welds modelled by modified **Gurson model**
KL Nielsen, V Tvergaard - Engineering Fracture Mechanics, 2010 - Elsevier
For resistance spot welded shear-lab specimens, interfacial failure under ductile shearing or ductile plug failure are analyzed numerically, using a shear modified **Gurson model**. The interfacial shear failure occurs under very low stress triaxiality, where the original **Gurson** ...
Cited by 162 Related articles All 5 versions Web of Science: 129 Import into BibTeX
[HTML] sciencedirect.com
Columbia e-link >>

Related searches

gurson model **ductile fracture**
gurson model **failure**
complete gurson model
modified gurson model
gurson model **shear**
gurson model **void**
gurson model **numerical**
gurson model **abaqus**

When there are lots of new materials/microstructures/meta-mateirals discovered, how can the supply of model matches the demands?

What are the alternatives?

Classical "recurrent" black-box architectures

Strain history
↓
GRU Layer
GRU Layer
↓
Flatten
↓
Dense
Dense
↓
Current stress

GRU Recurrent NN

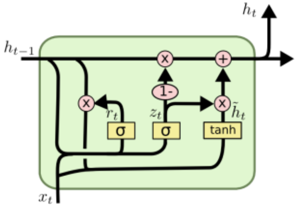

Current strain / Previous timestep stress
↓
Dense
Dense
Dense
↓
Current stress

Multi-step Feed-forward NN

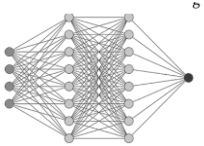

Strain history
↓
CONV1D Layer
CONV1D Layer
↓
Flatten / Pooling
↓
Dense
Dense
↓
Current stress

CONV1D Recurrent NN

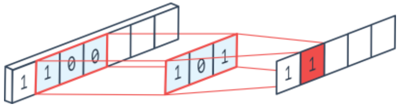

Our approach:

strain tensor

ϵ

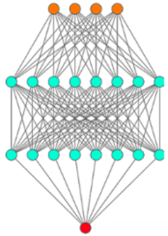

$\hat{\psi}$

Energy functional

Lode's coordinates and plastic strain

$\rho, \theta, \overline{\epsilon_p}$

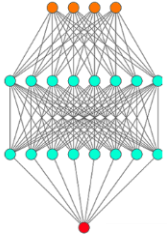

$\hat{f}$

Yield function

Higher-order Sobolev training - Higher-order activation functions.

- **Two neural networks** – hyperelastic energy functional and yield function.
- **Elastic** and **plastic** behaviors **decomposed**.
- Utilize plasticity theory to combine the two networks (**return mapping algorithm**)

Results for unseen cyclic loading data

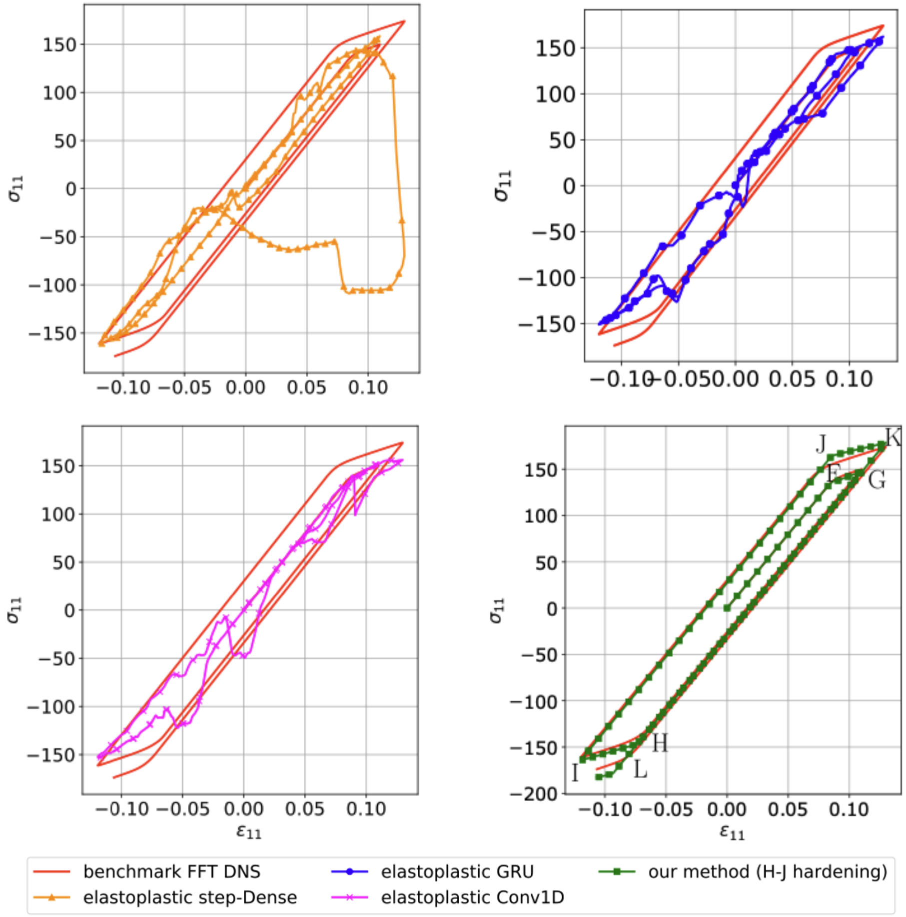

- A **classical machine learning** approach to predict **path-dependent elastoplasticity** behaviors uses **recurrent architectures** that are usually **black-box** and fail to predict unseen unloading paths
- We leverage classical plasticity theory to make **interpretable predictions even on unseen loading paths**.

Machine learning with sub-goals -- Identification of initial yield surface using elasticity model

Initial yield point

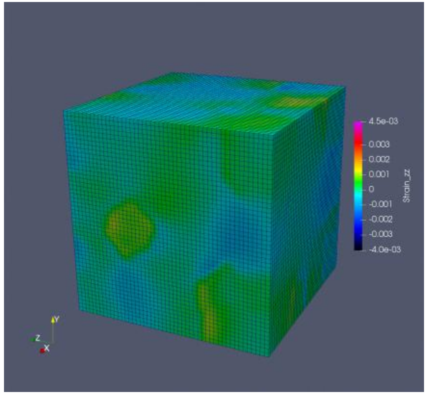

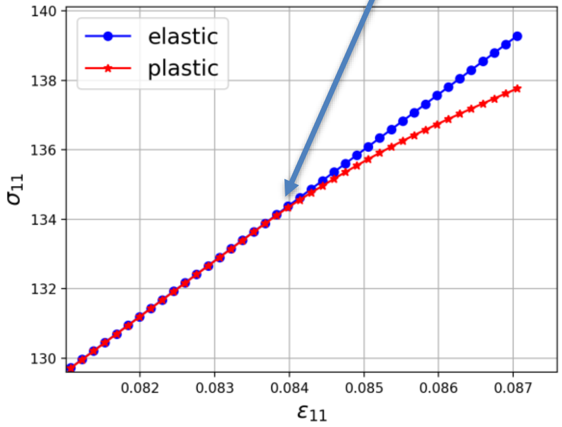

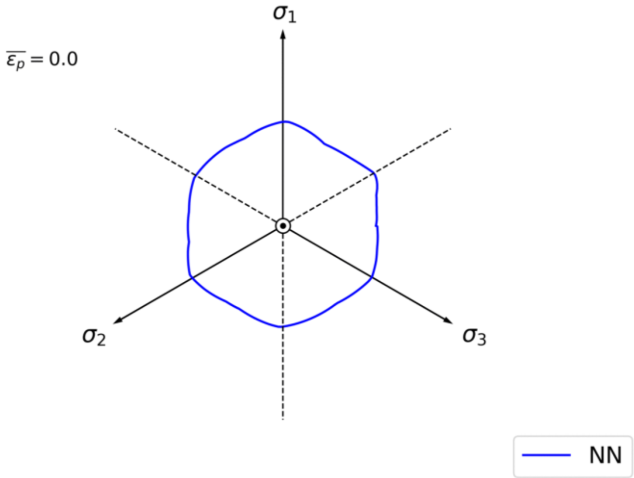

RVE simulations or experiments (w FFT solver)

Identify initial yield surface and hardening

Sobolev training for yield function

Converting yield surface into a signed distance function

Preprocess data as a level set initialization problem

1. Reduce dimensionality with **π-plane**:

$$x(\sigma_{11},\sigma_{22},\sigma_{33},\sigma_{12},\sigma_{23},\sigma_{13}) = \overline{x}(\sigma_1,\sigma_2,\sigma_3) = \widehat{x}(\rho,\theta).$$

2. Convert yield function into signed distance function by solving **Eikonal equation** in polar coordinates while enforcing the boundary f=0

$$|\nabla^{\widehat{x}}\phi| = 1 \longrightarrow (\frac{\partial\phi}{\partial\rho})^2 + \frac{1}{\rho^2}(\frac{\partial\phi}{\partial\theta})^2 = 1.$$

3. The resultant yield surface becomes

$$\phi(\widehat{\mathbf{x}},t) = \begin{cases} d(\widehat{\mathbf{x}}) & \text{outside } f_\Gamma \text{(inadmissible stress)} \\ 0 & \text{on } f_\Gamma \text{(yielding)} \\ -d(\widehat{\mathbf{x}}) & \text{inside } f_\Gamma \text{ (elastic region)} \end{cases},$$

where

$$d(\widehat{x}) = \min\left(|\widehat{x} - \widehat{x}_\Gamma|\right).$$

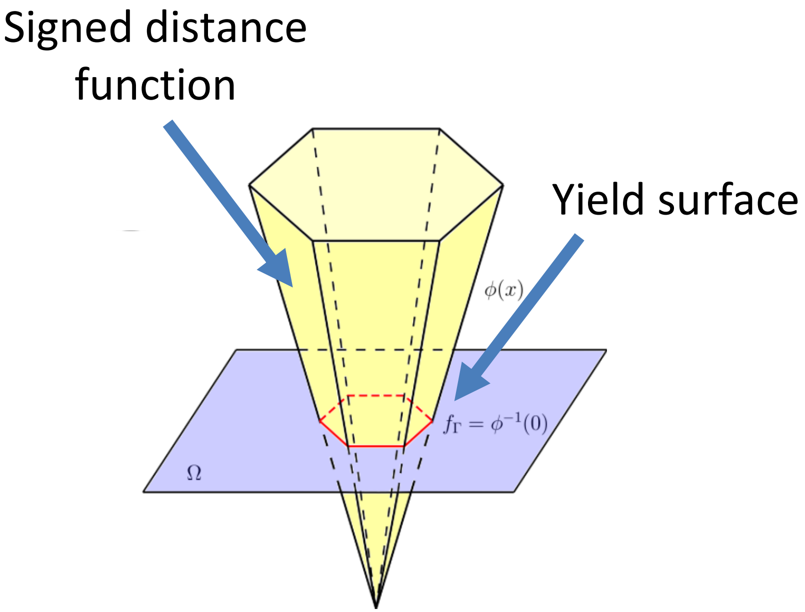

Benchmark Study: Predicting hardening/softening mechanism for pressure-dependent materials via ONE unified level set model

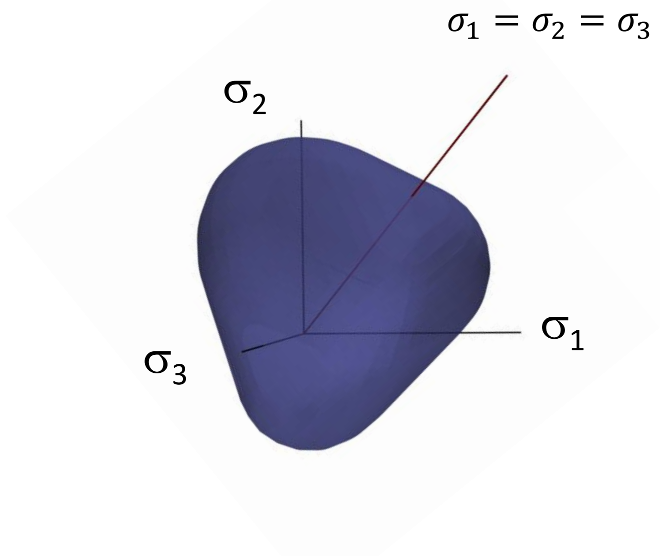

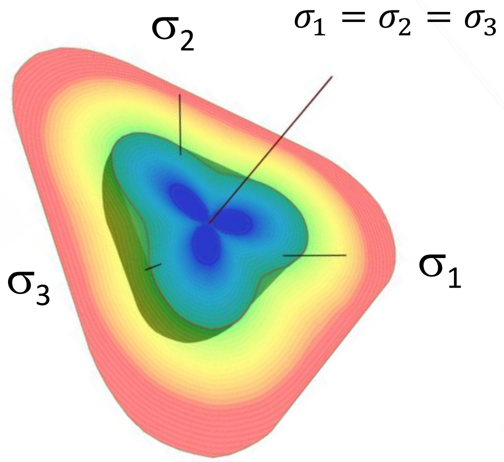

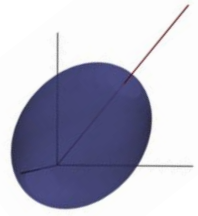

Isotropic hardening

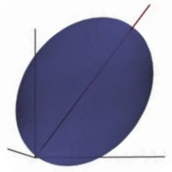

Kinematic hardening

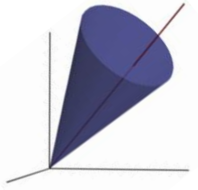

Rotational hardening

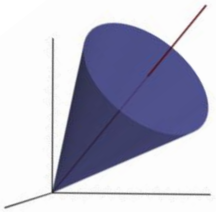

Frictional hardening

- Algorithm is readily **generalizable for pressure dependent models**
- Data-driven formulation any capture any form of hardening (isotropic, kinematic – change of **size** / **shape** / **translation** / **rotation** of yield surface in 3D stress space)

Extension 1: pressure-dependent models

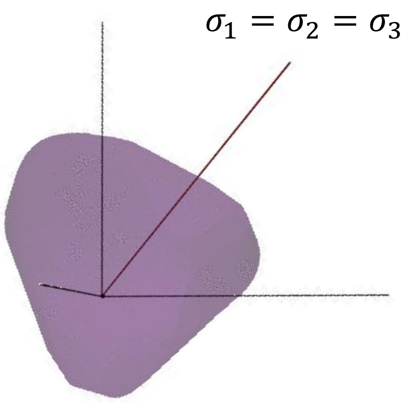

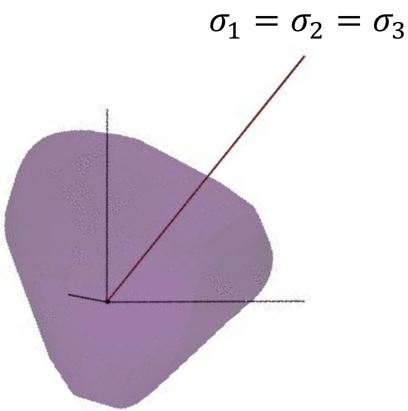

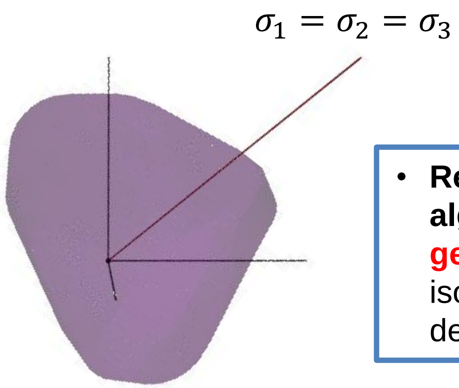

- **Return mapping algorithm** currently **generalizable** for isotropic pressure-dependent models

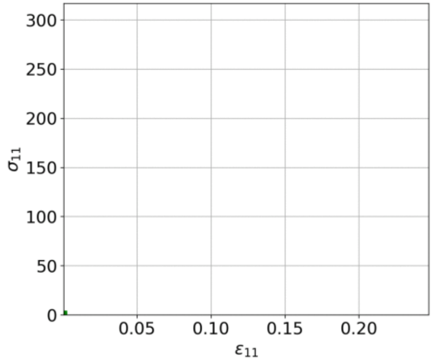

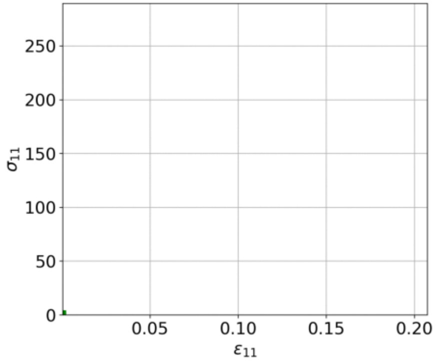

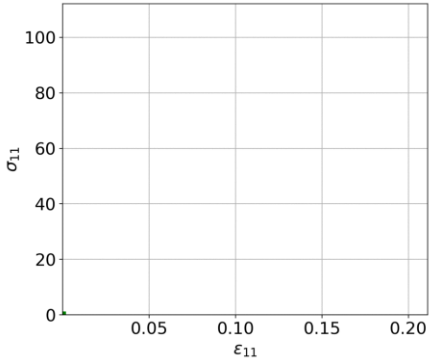

Capture complex hardening mechanisms

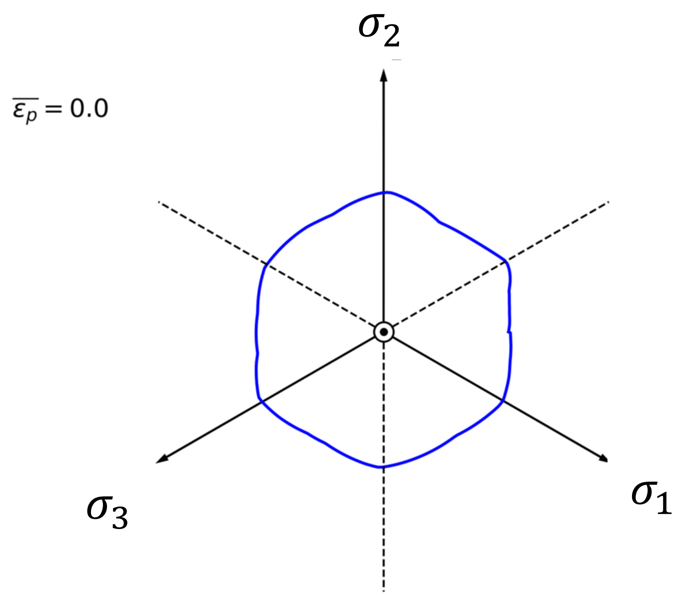

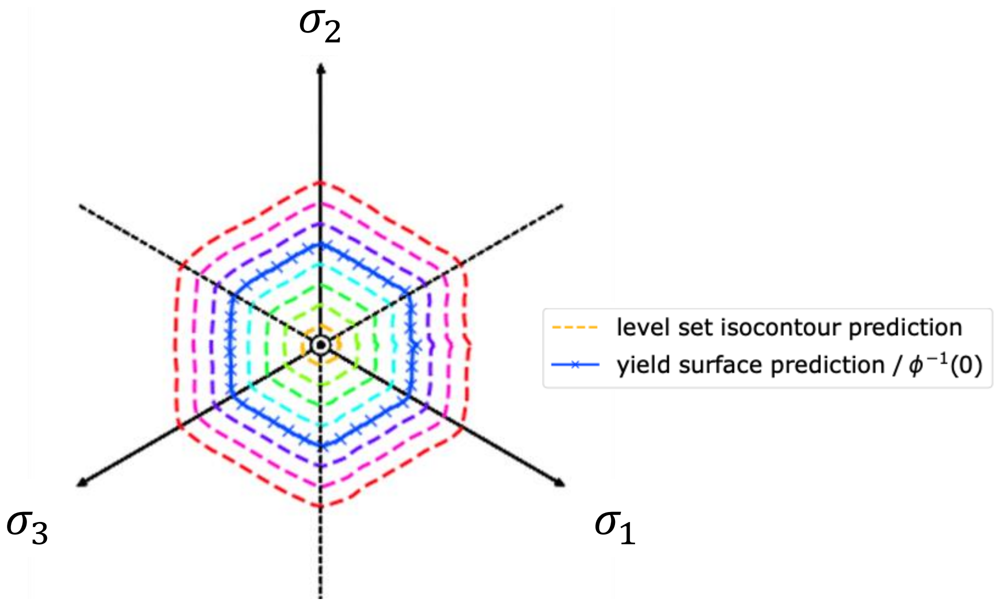

- The yield function function neural network can **capture a complex yield surface evolution** and **predict the entire level set** for an internal variable value (accumulated plastic strain $\overline{\epsilon_p}$).

ML-predicted dissipation and plastic flow direction

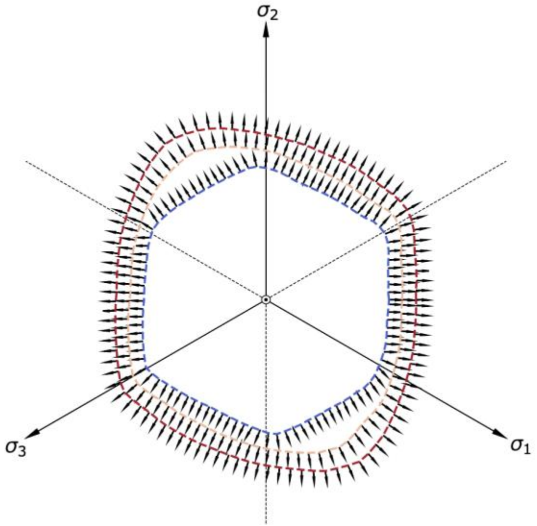

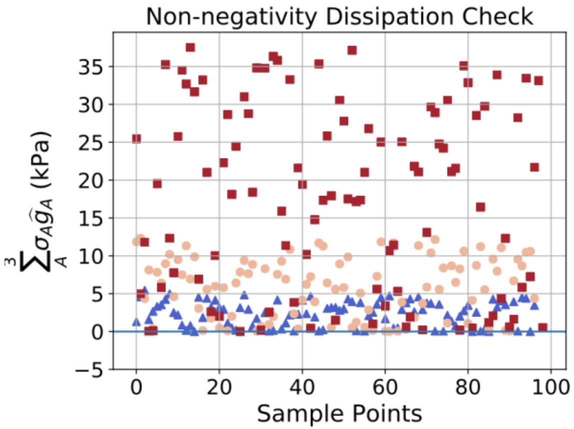

(a)

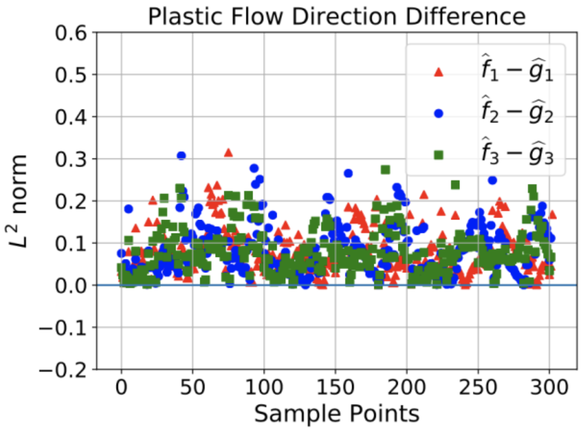

(b)

Vlassis & Sun, CMAME 2021

Elastoplasticity NN Framework – Polycrystal Plasticity Benchmark

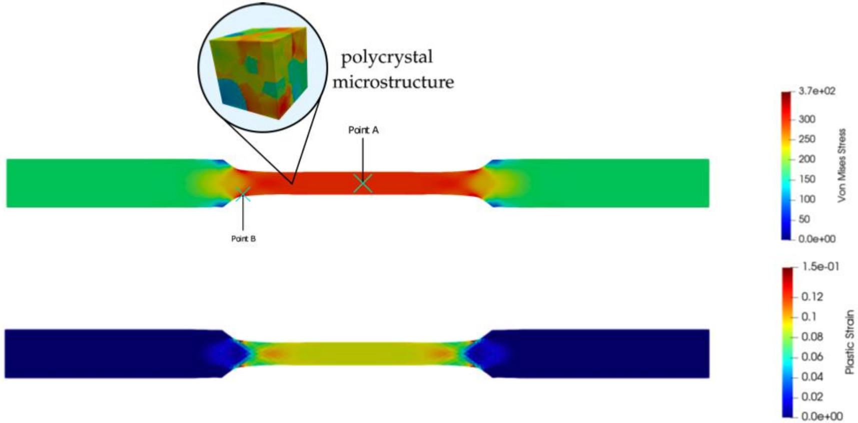

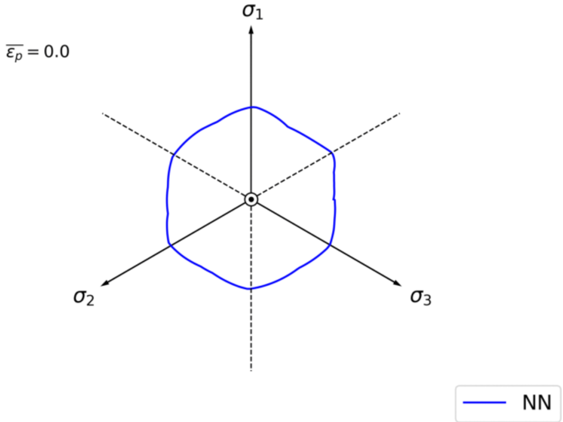

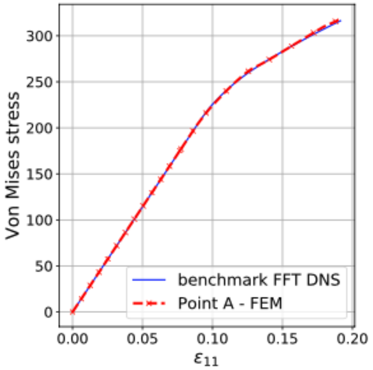

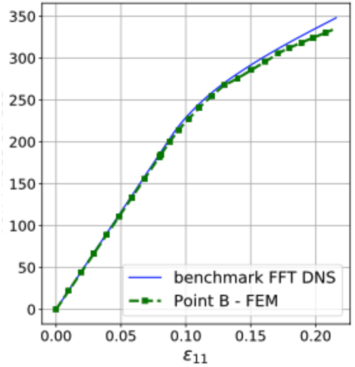

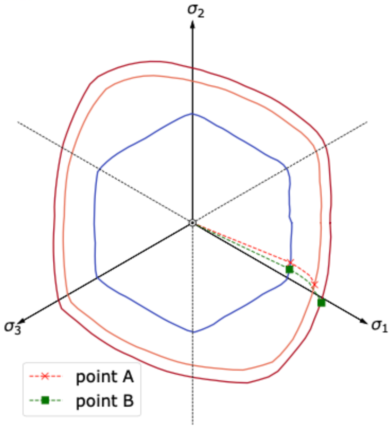

- **Polycrystal yield function** discovered from data – no need for complex yield function shape descriptors.
- Neural networks can **fully replace the elastoplastic constitutive model** – replace heavy FFT simulations at every material point.

Highlight 2: ***Geometric*** *learning for mechanics*

Graphs as microstructural representations

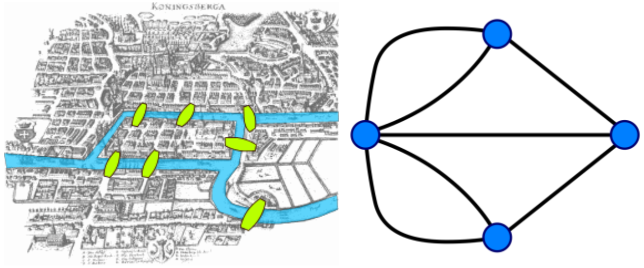

Euler's 1736 Königsberg Bridge problem

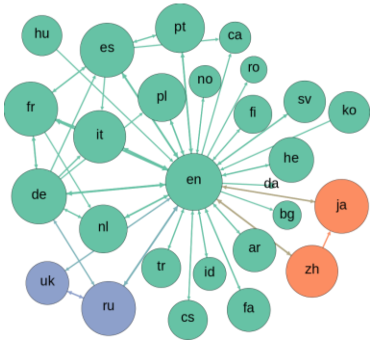

Wikipedia citation network

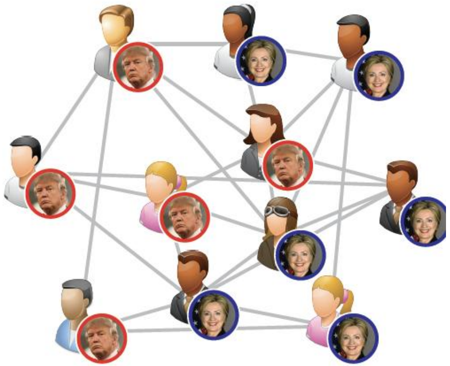

Predictions on social network

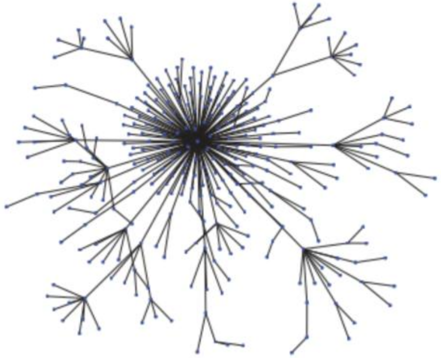

Fake news detection

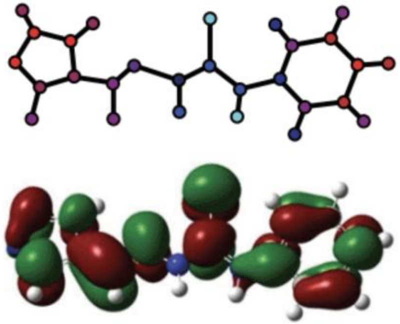

Chemistry

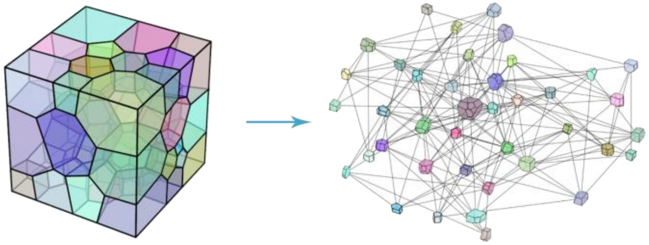

Microstructures

Future Work: Geometric learning for evolving connectivity graphs

- Stress evolutions under various loadings (grain scale)

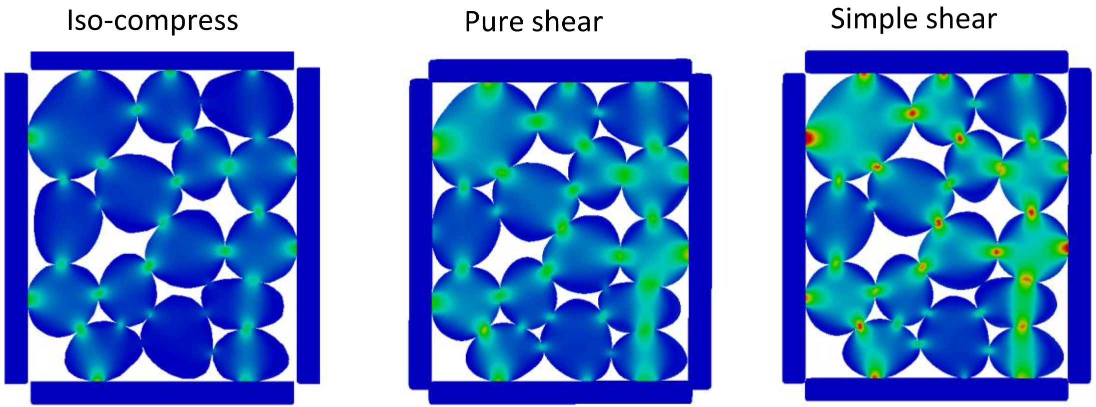

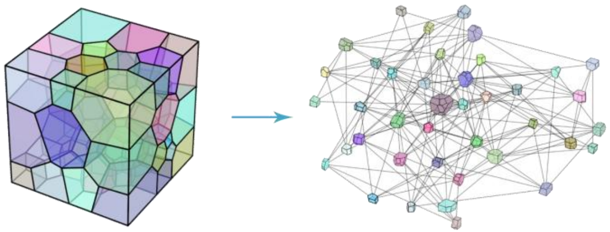

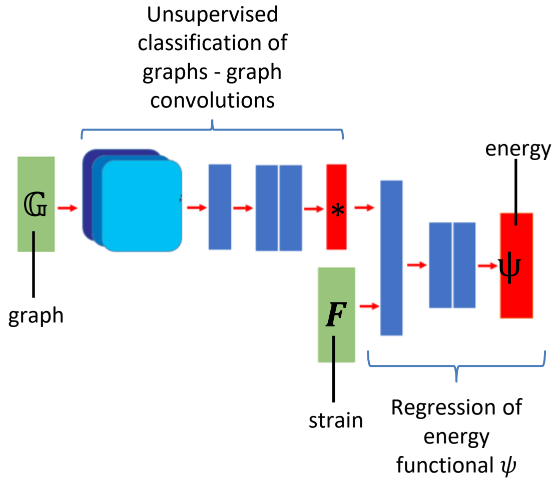

Creating low-dimensional representation graph to represent microstructures from voxel images

Vlassis, Ma & Sun, CMAME 2020

(For convolutional neural network on voxel images, see Frankel et al, CMS 2019)

C. Liu", **W.C. Sun**, ILS-MPM: an unbiased implicit level-set-based material point method for frictional particulate contact mechanics of deformable particles, *Computer Methods in Applied Mechanics and Engineering*, , doi:10.1016/j.cma.2020.113168, 2020.

Step 1B: Undirected weighted graphs as low-dimensional representation of microstructures

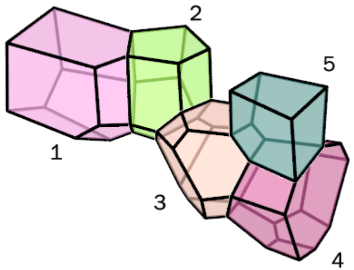

Polycrystal formation (often high-dimensional voxel images)

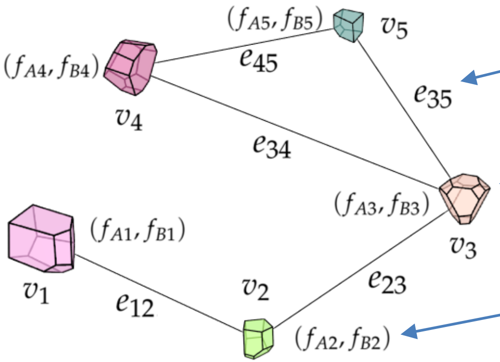

Undirected weighted (connectivity) graph (n-tuple)

- Two crystals that are in contact are connected by an **edge**

- Every crystal is a **node**

- Every node has **weights – features**

[volume, orientation, number of neighbors, number of edges, number of surfaces, etc.]

In the above example:

$$\mathbb{V} = \{v_1, v_2, v_3, v_4, v_5\}$$

$$\mathbb{E} = \{e_{12}, e_{23}, e_{34}, e_{35}, e_{45}\}$$

Vertex and edge sets

$$\boldsymbol{D} = \begin{bmatrix} 1 & 0 & 0 & 0 & 0 \\ 0 & 2 & 0 & 0 & 0 \\ 0 & 0 & 3 & 0 & 0 \\ 0 & 0 & 0 & 2 & 0 \\ 0 & 0 & 0 & 0 & 2 \end{bmatrix}$$

Degree (of connectivity)

$$\boldsymbol{A} = \begin{bmatrix} 0 & 1 & 0 & 0 & 0 \\ & 0 & 1 & 0 & 0 \\ & & 0 & 1 & 1 \\ & & & 0 & 1 \\ \text{sym.} & & & & 0 \end{bmatrix}$$

adjacency matrix

$$\boldsymbol{L} = \begin{bmatrix} 1 & -1 & 0 & 0 & 0 \\ & 2 & -1 & 0 & 0 \\ & & 3 & -1 & -1 \\ & & & 2 & -1 \\ \text{sym.} & & & & 2 \end{bmatrix}$$

Graph Laplacian

$$\boldsymbol{L} = \boldsymbol{D} - \boldsymbol{A},$$

$$\boldsymbol{L}^{\text{sym}} = \begin{bmatrix} 1 & -\frac{\sqrt{2}}{2} & 0 & 0 & 0 \\ -\frac{\sqrt{2}}{2} & 1 & -\frac{\sqrt{6}}{6} & 0 & 0 \\ 0 & -\frac{\sqrt{6}}{6} & 1 & -\frac{\sqrt{6}}{6} & -\frac{\sqrt{6}}{6} \\ 0 & 0 & -\frac{\sqrt{6}}{6} & 1 & -\frac{1}{2} \\ 0 & 0 & -\frac{\sqrt{6}}{6} & -\frac{1}{2} & 1 \end{bmatrix}$$

Symmetric normalized graph Laplacian

$$\boldsymbol{L}^{\text{sym}} = \boldsymbol{D}^{-\frac{1}{2}} \boldsymbol{L} \boldsymbol{D}^{-\frac{1}{2}}$$

$$\boldsymbol{X} = \begin{bmatrix} f_{A1} & f_{B1} \\ f_{A2} & f_{B2} \\ f_{A3} & f_{B3} \\ f_{A4} & f_{B4} \\ f_{A5} & f_{B5} \end{bmatrix}$$

Feature matrix (e.g. Euler angle, size of grain, ..etc)

Vlassis, Ma & Sun, under review

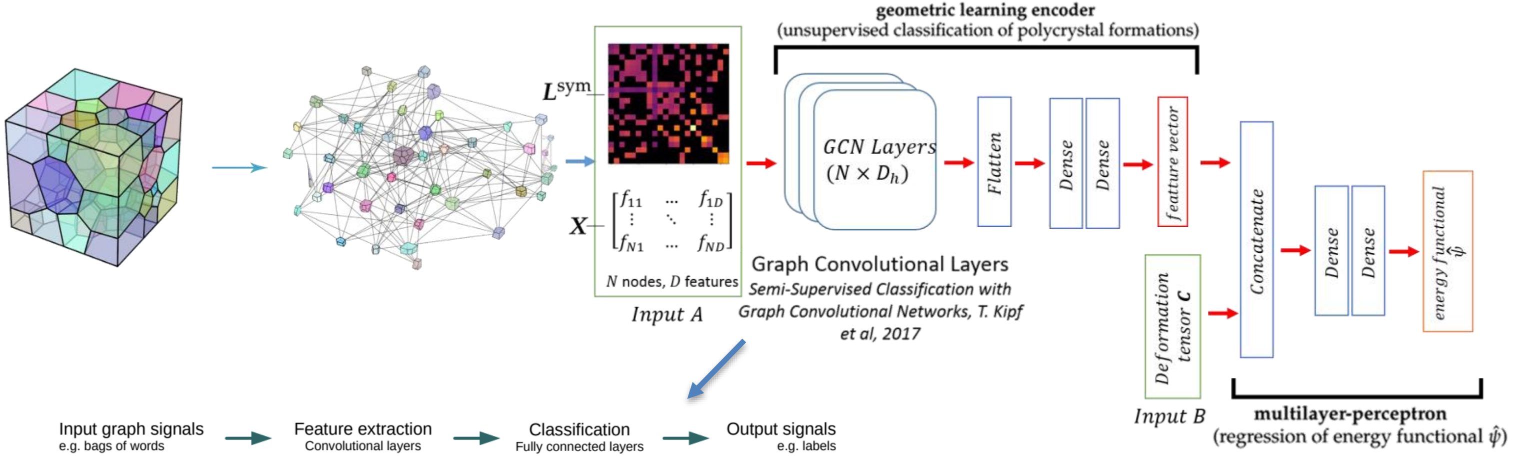

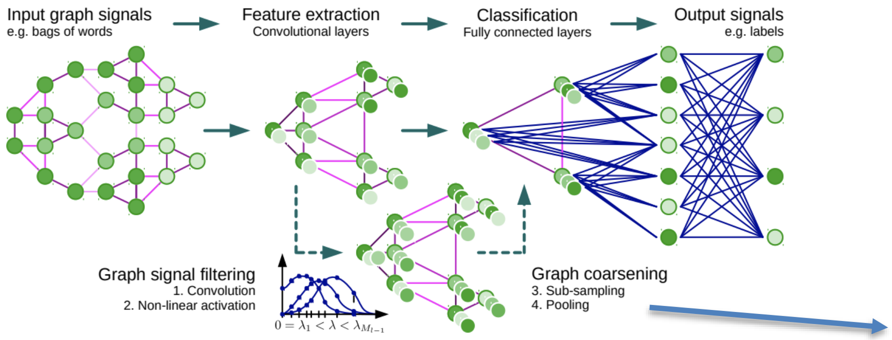

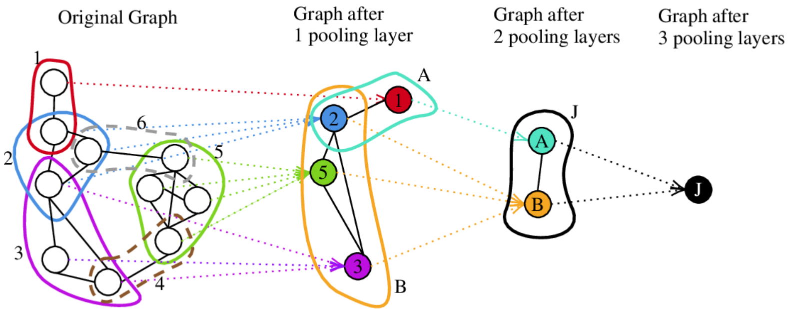

Figure taken from Defferrard, Bresson, Pierre Vandergheynst (NIPS 2016).

Vlassis, Ma & Sun, CMAME, 2020

Figure from Luzhnica, Bay, Lio (ICLR 2019).

Isotropic Elasticity L_2 norm - H_1 norm Training Comparison

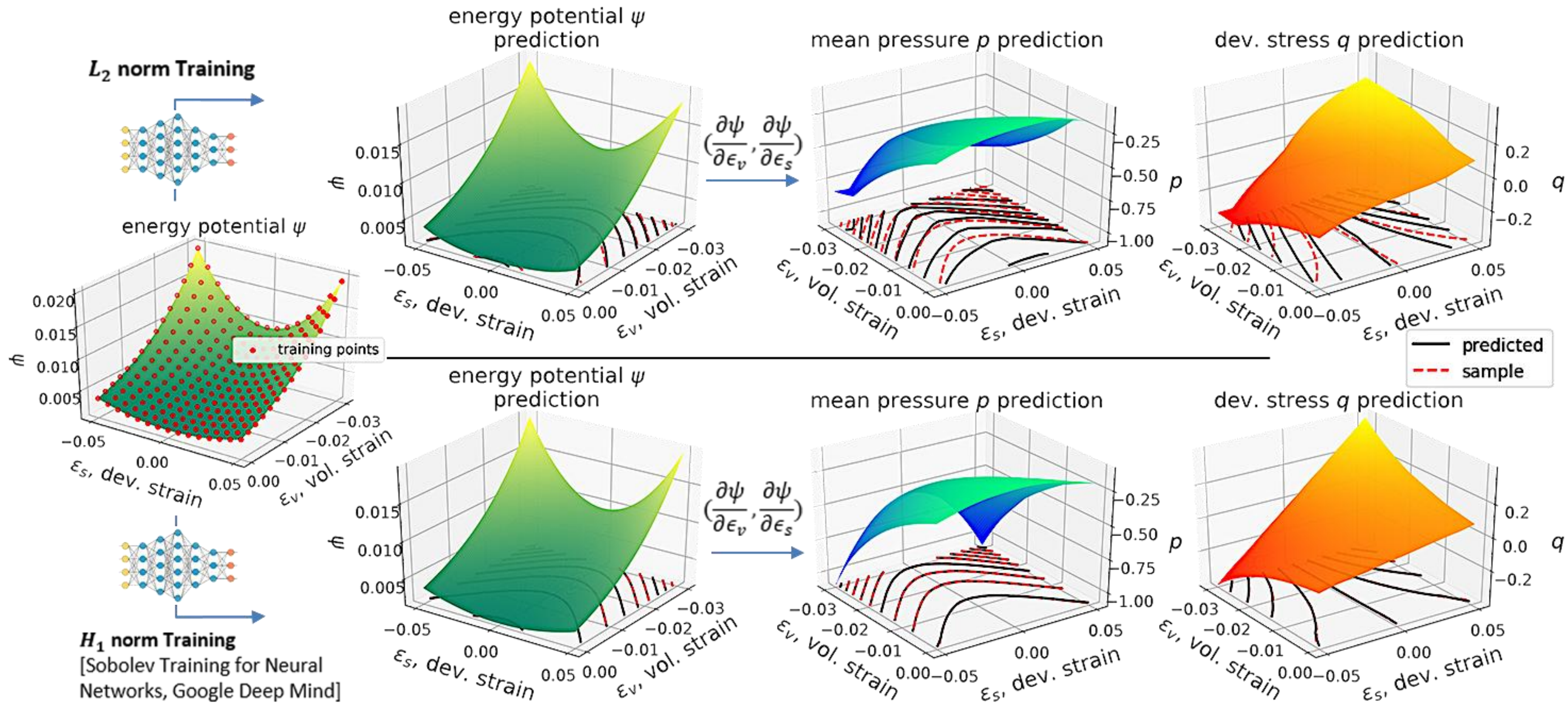

Vlassis, Ma & Sun, under review

Predictions of polycrystal elasticity for calibrated and unseen RVEs

Predictions of elastic responses on unseen RVEs

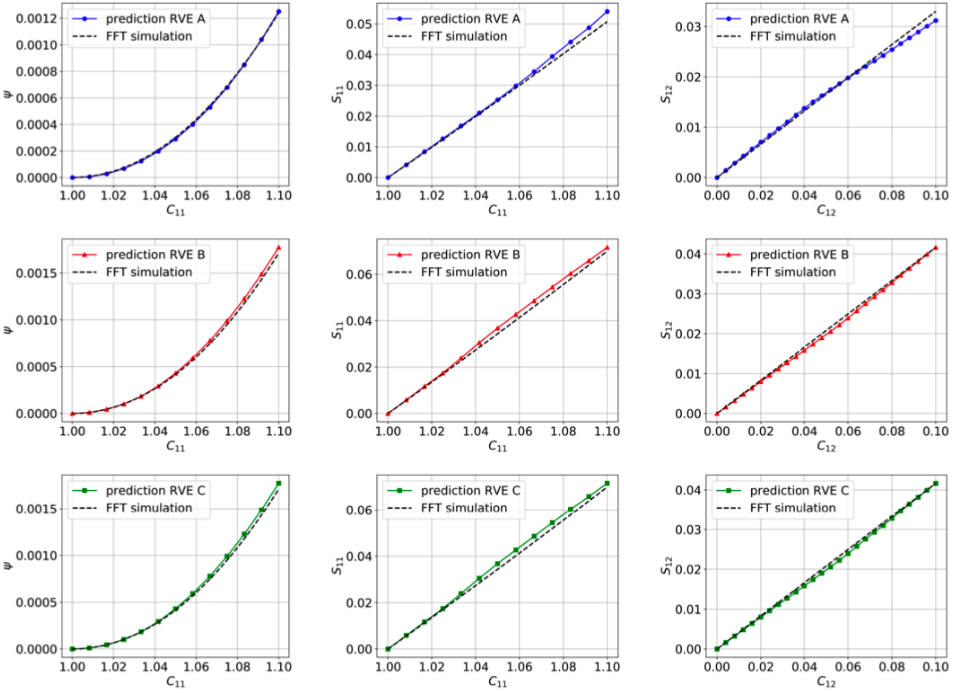

Graph isomorphism test

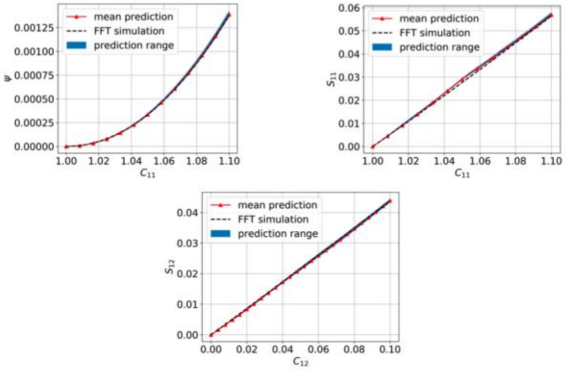

Convexity test

$$\hat{\psi}(\mathbf{C}_\alpha, \mathrm{G}_k) \geq \hat{\psi}(\mathbf{C}_\beta, \mathrm{G}_k) + \frac{\partial \hat{\psi}}{\partial \mathbf{C}}(\mathbf{C}_\beta, \mathrm{G}_k) : (\mathbf{C}_\alpha - \mathbf{C}_\beta), \quad \text{for all} \quad \mathbf{C}_\alpha, \mathbf{C}_\beta \in D \text{ and } k \in [1, ..., N_{RVE}]$$

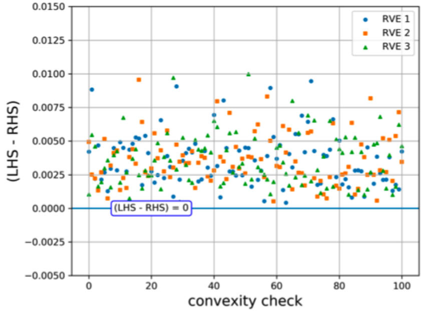

Vlassis, Ma & Sun, under review

Ongoing work: Equivariant Geometric Learning/Graph Convolutional Neural Network for mechanics problems

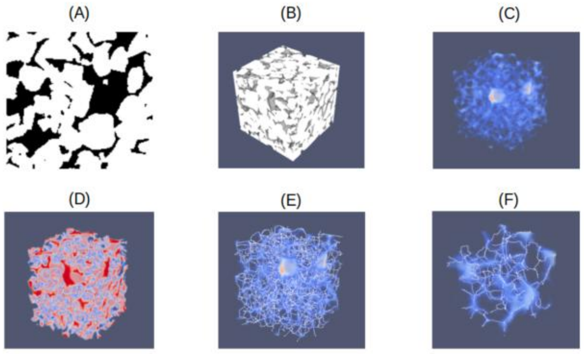

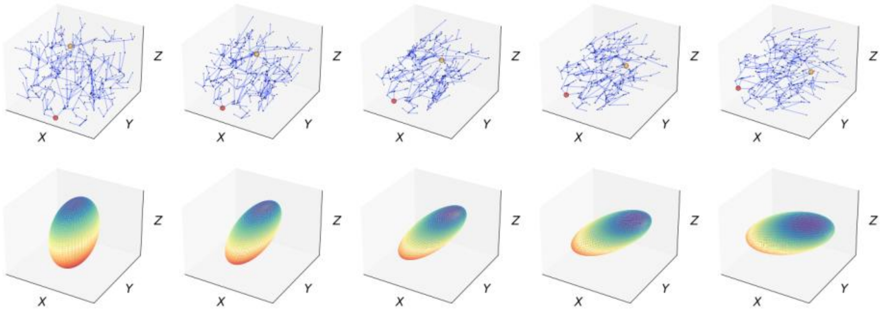

1. Data compression with non-Eucidean space

2. Use Equivariant neural network to enforce material frame indifference (i.e. predictions not depend on observers)

seed	CNN	GNN	Equivariant GNN	Improvement
1	0.081	0.048	0.039	17.6%
2	0.091	0.049	0.044	9.9%
3	0.129	0.050	0.043	14.6%
4	0.127	0.051	0.042	18.3%
5	0.151	0.047	0.039	17.4%
mean	0.116	0.049	0.041	15.6%

In collaboration with Yusu Wang UCSD supported by NSF IDEA LABS

Future/Ongoing Work: Causal Discovery for Traction Separation Law
(Collaboration with Yanxun Xu group from Johns Hopkins)

- **Background:** Traction-Separation Law generated by reinforcement learning
- **Challenge:** Deterministic predictions are insufficient for cases with aleatoric and epistemic uncertainties
- **Objective:** To develop the new algorithm for efficient predictions that propagate uncertainties
- **Method**: Utilizing the **Causal Discovery, Ensemble learning and Uncertainty Quantification** to improve the predicted mechanics laws

Procedures:

Graph generated by causal discovery algorithm

e
g:

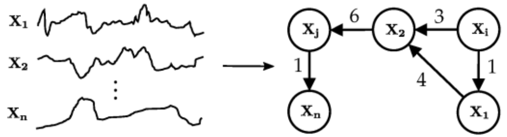

Edge in graphs lead to supervised learning that employs dropout GRU network as well as Ensemble

e
g:

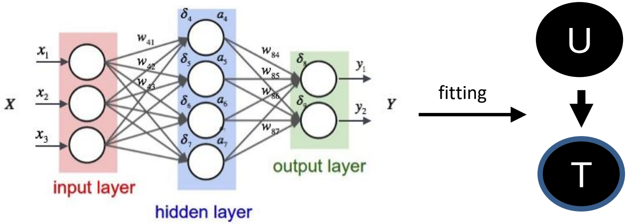

Uncertainty predictions by MCMC

e
g:

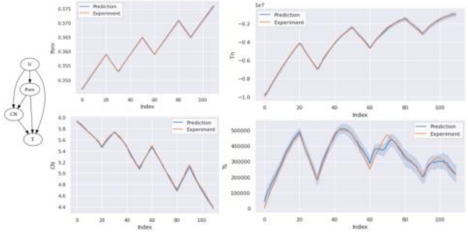

Sun et al. under review at Granular Matter

Highlight 3: Validation through competitions: non-cooperative game for experiment design

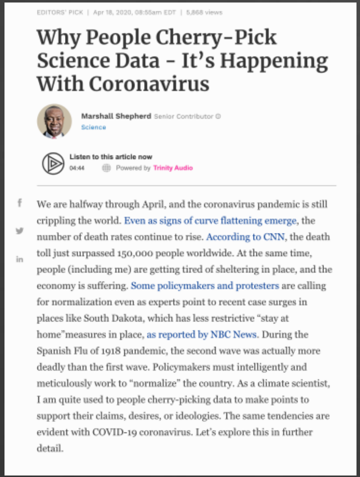

EDITORS' PICK | Apr 18, 2020, 08:55am EDT | 5,868 views

Why People Cherry-Pick Science Data – It's Happening With Coronavirus

Marshall Shepherd Senior Contributor
Science

Listen to this article now
04:44 Powered by Trinity Audio

We are halfway through April, and the coronavirus pandemic is still crippling the world. Even as signs of curve flattening emerge, the number of death rates continue to rise. According to CNN, the death toll just surpassed 150,000 people worldwide. At the same time, people (including me) are getting tired of sheltering in place, and the economy is suffering. Some policymakers and protesters are calling for normalization even as experts point to recent case surges in places like South Dakota, which has less restrictive "stay at home"measures in place, as reported by NBC News. During the Spanish Flu of 1918 pandemic, the second wave was actually more deadly than the first wave. Policymakers must intelligently and meticulously work to "normalize" the country. As a climate scientist, I am quite used to people cherry-picking data to make points to support their claims, desires, or ideologies. The same tendencies are evident with COVID-19 coronavirus. Let's explore this in further detail.

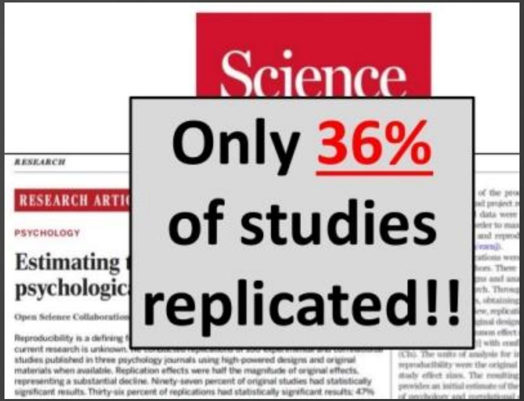

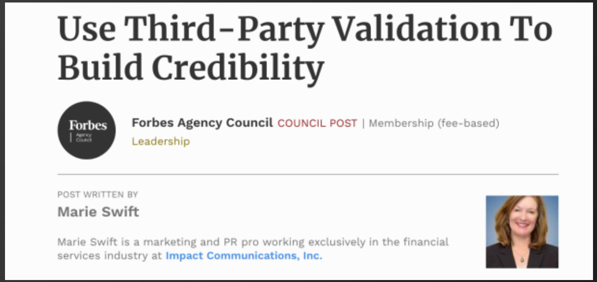

Use Third-Party Validation To Build Credibility

Forbes Agency Council COUNCIL POST | Membership (fee-based)
Leadership

POST WRITTEN BY
Marie Swift

Marie Swift is a marketing and PR pro working exclusively in the financial services industry at Impact Communications, Inc.

Deep reinforcement learning for decision-making during modeling

Alpha Go Zero

Legal game positions: 2e170 > atoms in universe 1.6e79

https://deepmind.com/blog/alphago-zero-learning-scratch/

3 hours

Beginner level with greedy plays

19 hours

Learnt the fundamentals of Go strategies

70 hours

Super-human level with disciplined plays

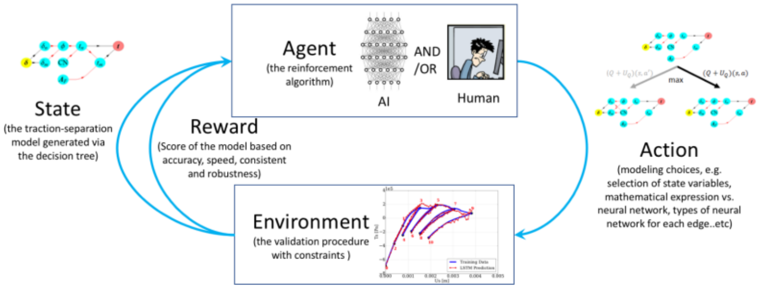

Meta modeling DRL

Legal game positions depend on the number of nodes of internal features

In our example: over 2e4

10 games

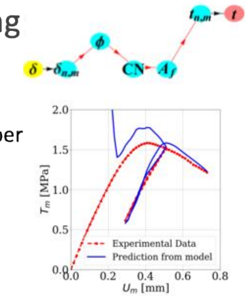

30 games

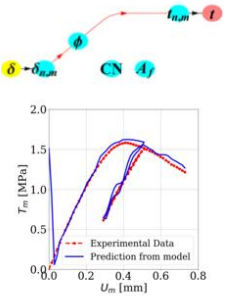

100 games

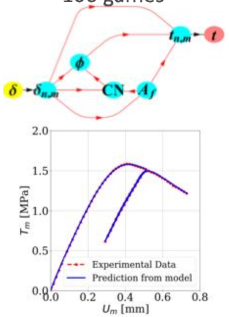

Environment	Idealized multigraph for constitutive models validated against unseen data
Agent	Human or AI
State s	The generated constitutive laws
Action a	The decisions that lead to the generation of constitutive laws
Reward r	Score (objective function) of the constitutive model
$v(s)$	Expected model score of state s
Q-value $Q(s,a)$	Expected model score from taking action a at state s
$\pi(s,a)$	Probability of taking action a at state s

Modeling game with classical descriptors in Euclidean space and Lie group (porosity, fabric tensor, coordination number, 3-cycle…etc, cf. Wang & Sun, CMAME, 2019; Wang, Sun, Du, CM, 2019) -- What about non-Euclidean data (graph, manifold?)

Training Example 1: Training traction-separation law from DEM simulations

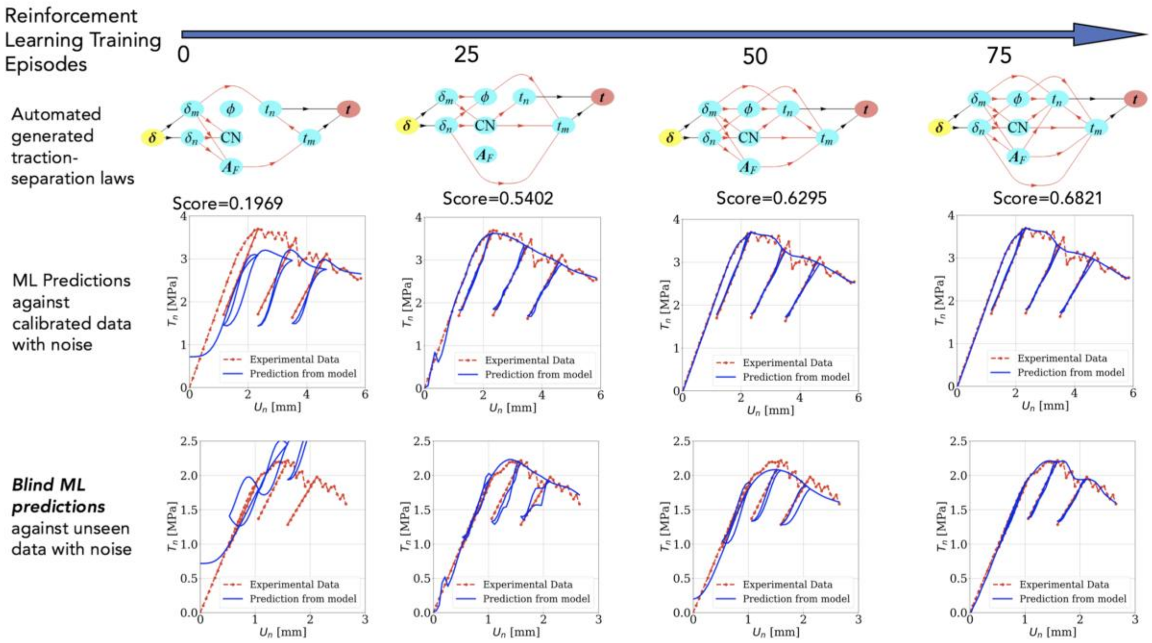

Figure 6: *Improved calibration and blind prediction scores throughout the training. As time progresses, the AI learn to write models with increasingly precise predictions. After 75 episodes (i.e. 75 different constitutive laws are built, both the calibration exercises and blind predictions (blue) are able to yield excellent matches with the benchmark (red).*

Wang & Sun, CMAME, 2019, Wang, Sun & Du, CM 2019

Here, our goal is to use DRL to design experiments to validate and **attack** of a model simultaneously …

Two-player non-cooperative game

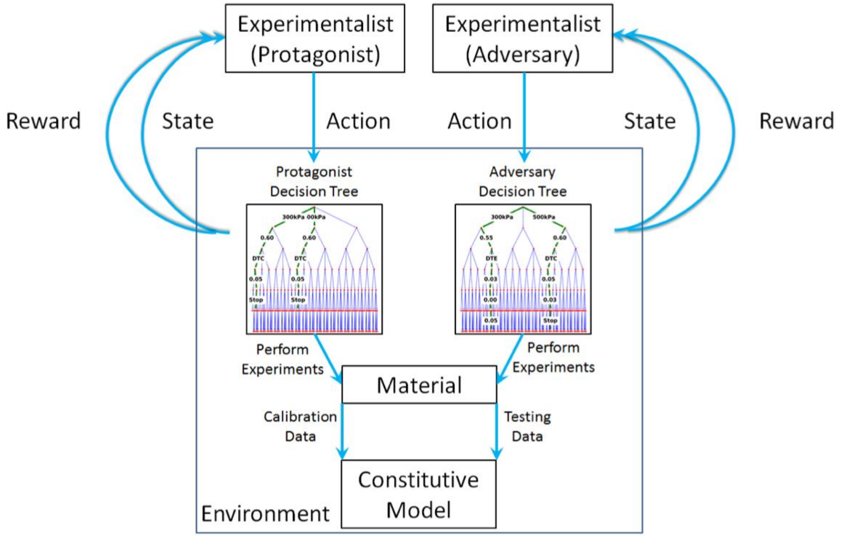

$$\mathrm{Reward}_{\mathrm{protagonist}} = +\mathrm{SCORE}_{\mathrm{protagonist}}.$$

$$\mathrm{Reward}_{\mathrm{adversary}} = -\mathrm{SCORE}_{\mathrm{adversary}}.$$

Wang, Sun & Du, under review

Possible applications represented by a polytree; an experiment becomes a walk.

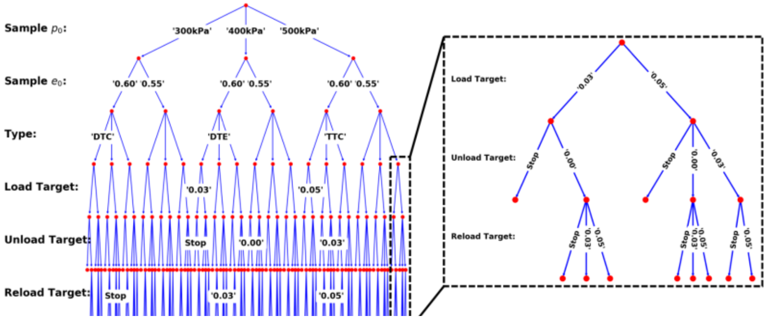

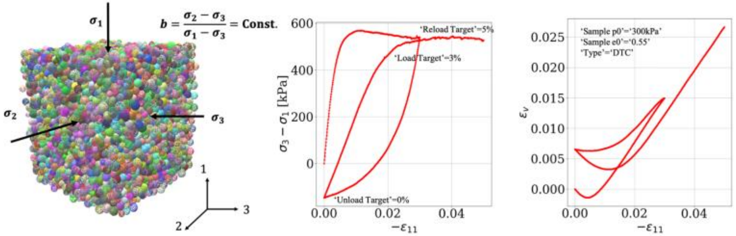

Conventionally, we rely on intuition and experiments to design experiments. Here, DRL is attempting to estimate the relative values of the tests to suggest experiments

Training of two-player adversarial reinforcement learning for optimal strategies to calibrate and falsify a constitutive law.

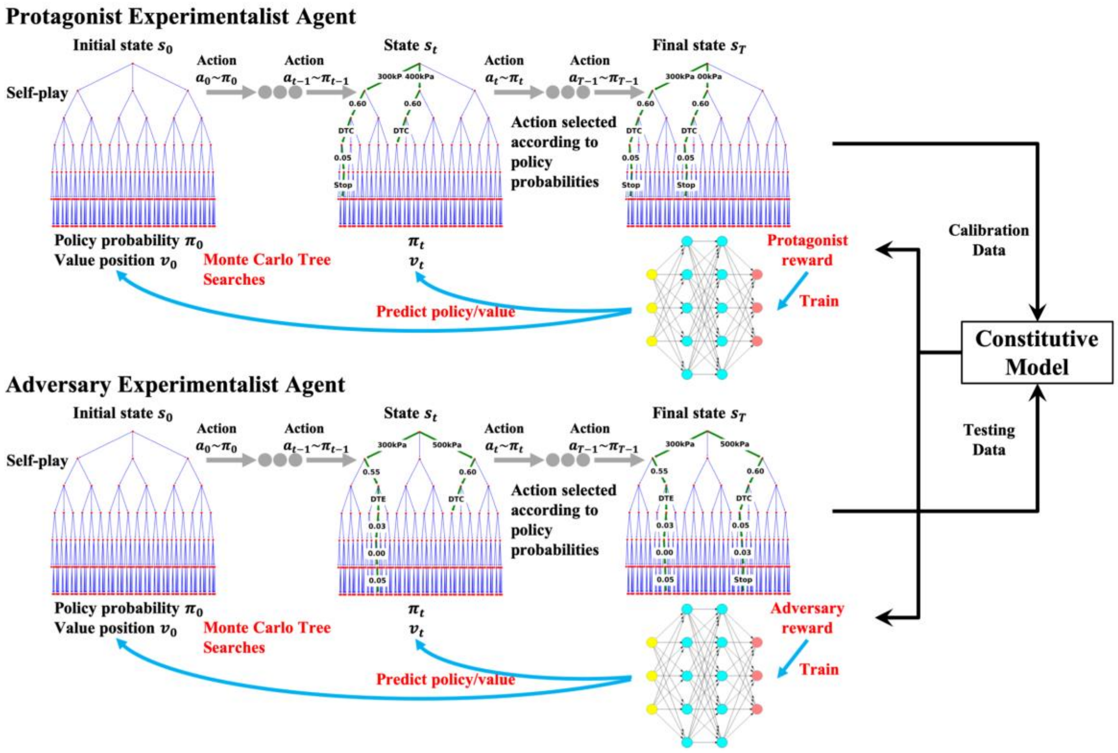

Agent 1 is tasked with generating new experiential data to calibrate a model.

Agent 2 try to undermine the calibration effort of Agent 1 by finding the tests that maximize the calibration errors

Self-play reinforcement learning for two competing agents.

In each “play”, reward is assessed, then the reward for each action is estimated.

If we know the true “reward” of each action, we can determine the optimal action sequence that yields the best model.

Neural network is used to estimate the value of each policy without hand-crafted evaluation functions (the same for AlphaGo Zero)

Wang, Sun & Du, under review

Training with parallel adversarial attack

DRL update Q values for each policy

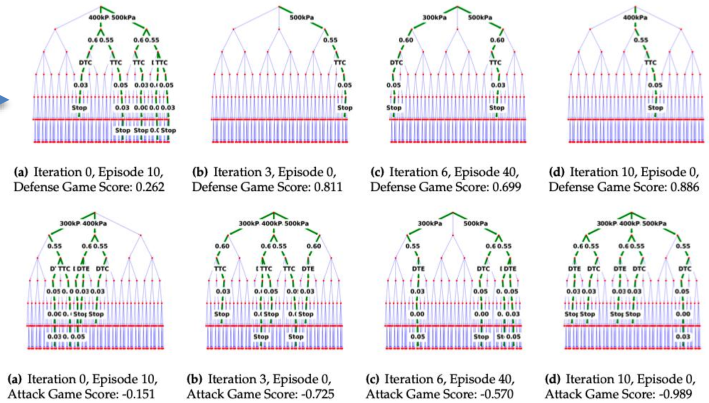

(a) Iteration 0, Episode 10, Defense Game Score: 0.262
(b) Iteration 3, Episode 0, Defense Game Score: 0.811
(c) Iteration 6, Episode 40, Defense Game Score: 0.699
(d) Iteration 10, Episode 0, Defense Game Score: 0.886

(a) Iteration 0, Episode 10, Attack Game Score: -0.151
(b) Iteration 3, Episode 0, Attack Game Score: -0.725
(c) Iteration 6, Episode 40, Attack Game Score: -0.570
(d) Iteration 10, Episode 0, Attack Game Score: -0.989

Run “Experiments”

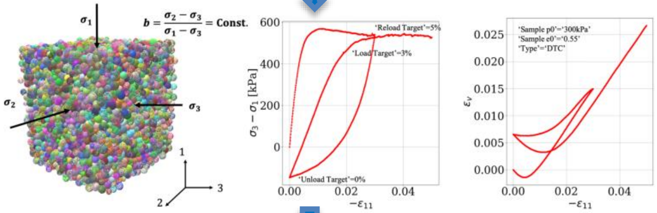

Calibrated by protagonist
Falsified by adversary

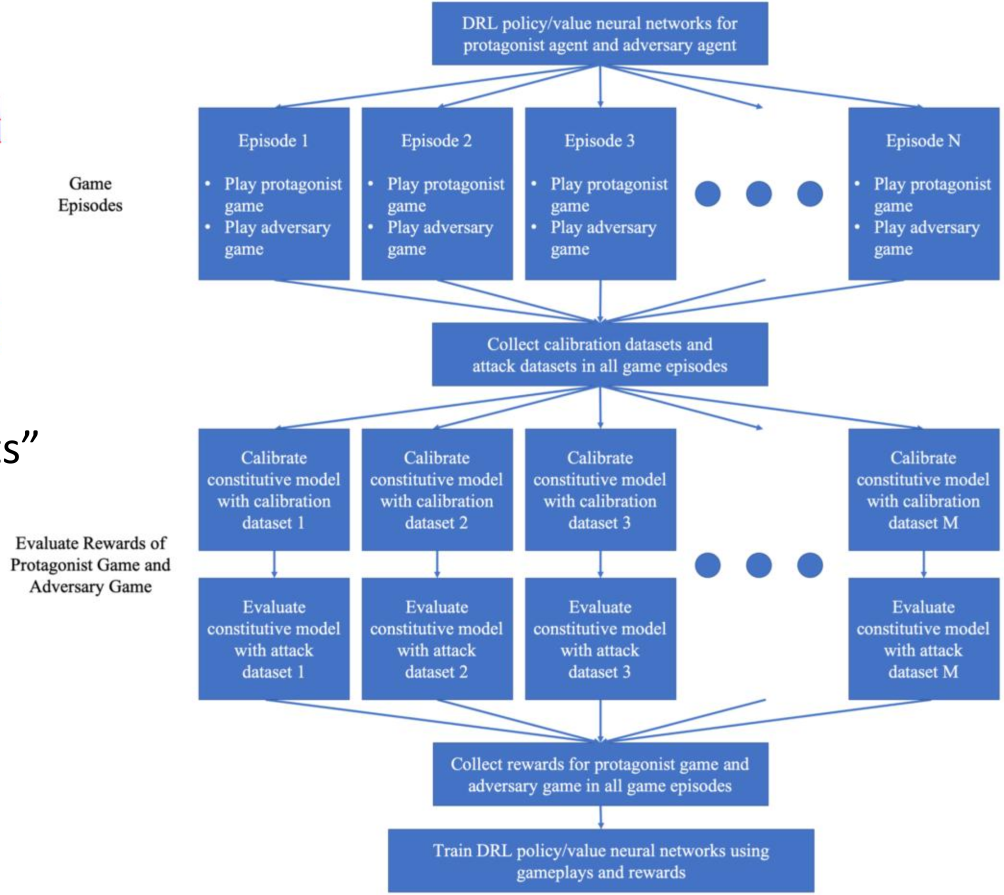

Game Play for the non-cooperative game

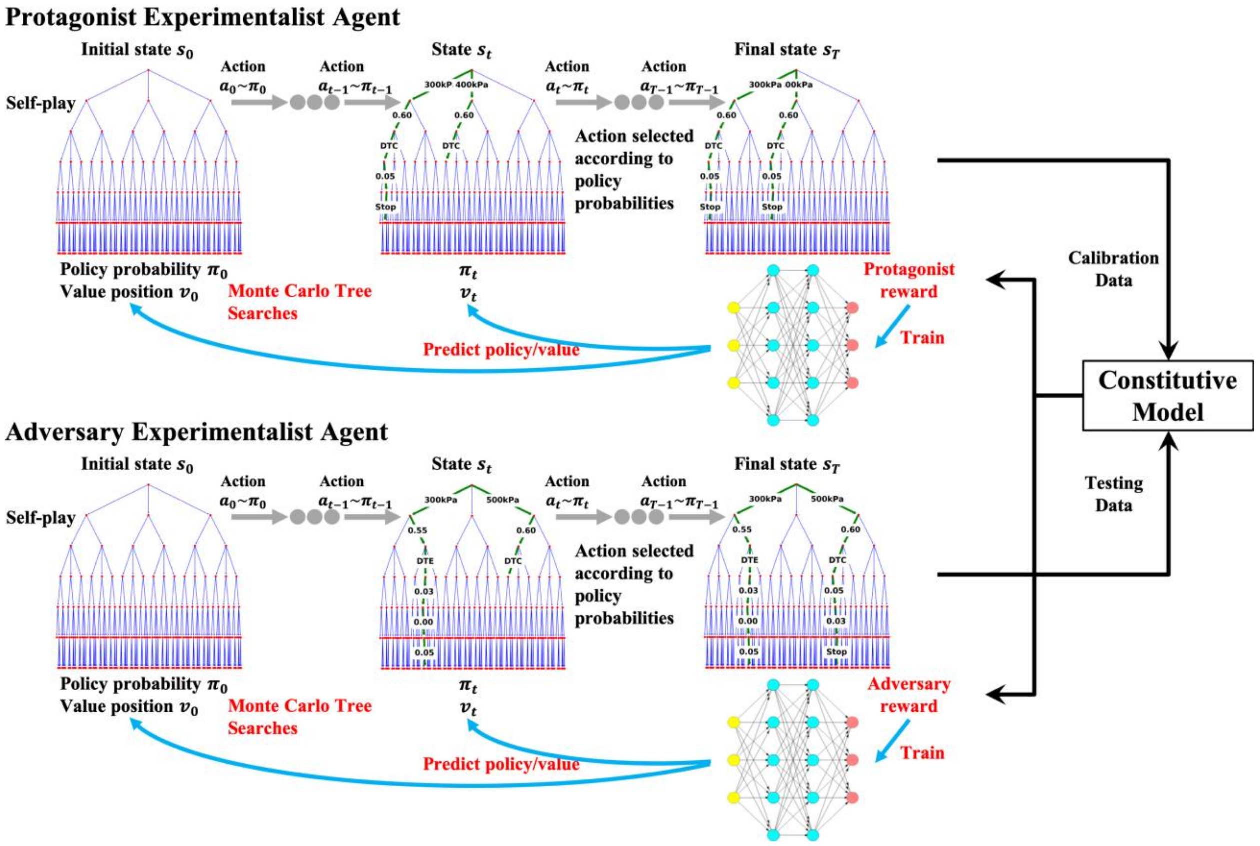

A non-cooperative meta-modeling game for automated third-party training, validating, and falsifying constitutive laws with adversarial attacks, CMAME, 2020.

Reinforcement learning performance of the experimentalist/adversary game (Drucker-Prager)

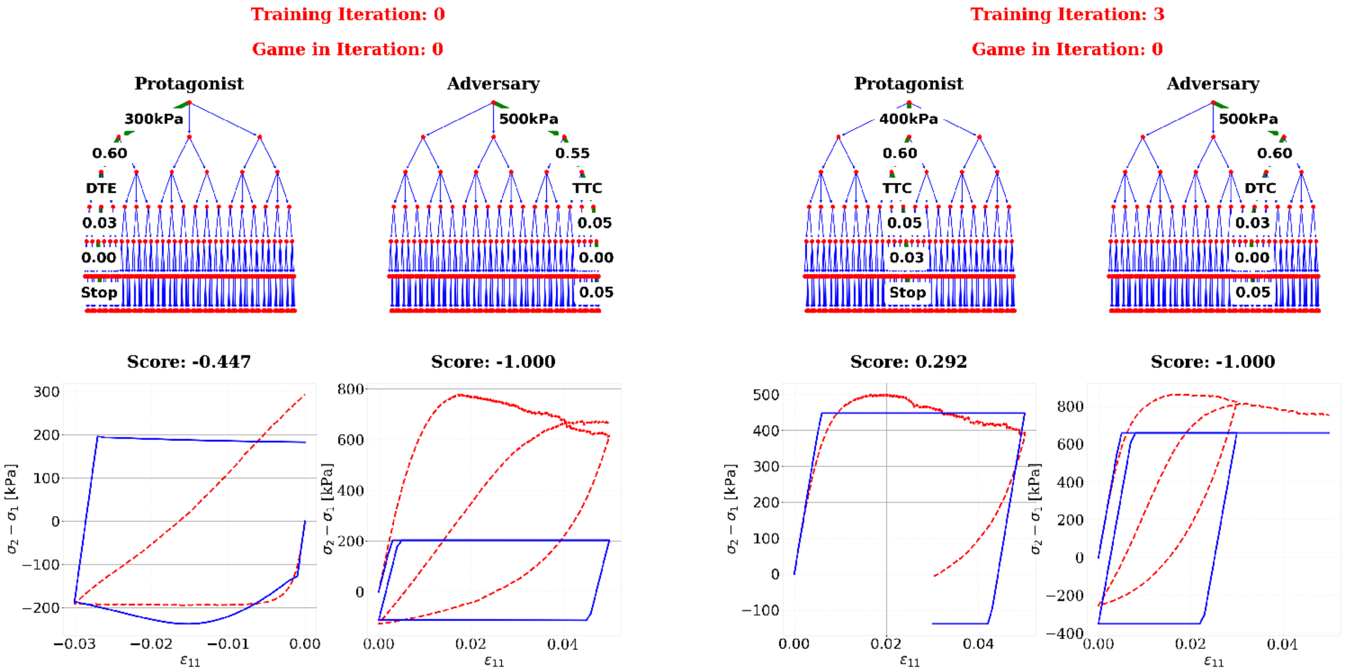

Initially, both agents are exploring the parametric space and attempt to improve their estimated Q values through interacting with each others.

Reinforcement learning performance of the experimentalist/adversary game (Bounding surface plasticity model)

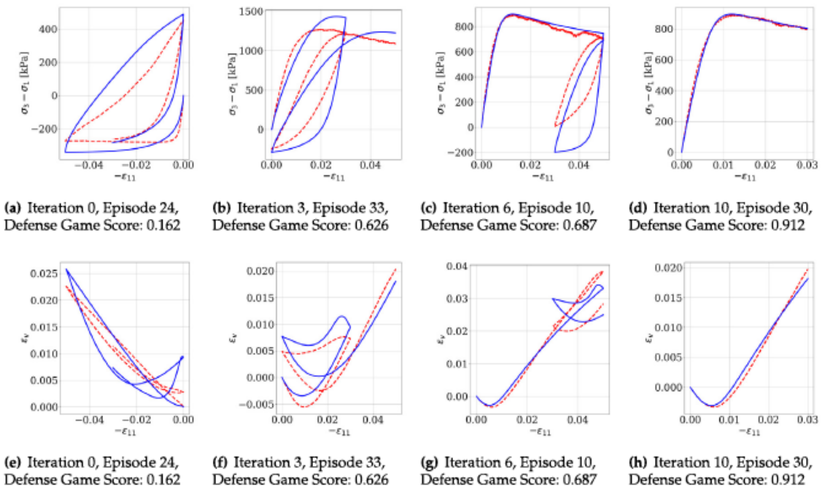

(a) Iteration 0, Episode 24, Defense Game Score: 0.162

(b) Iteration 3, Episode 33, Defense Game Score: 0.626

(c) Iteration 6, Episode 10, Defense Game Score: 0.687

(d) Iteration 10, Episode 30, Defense Game Score: 0.912

(e) Iteration 0, Episode 24, Defense Game Score: 0.162

(f) Iteration 3, Episode 33, Defense Game Score: 0.626

(g) Iteration 6, Episode 10, Defense Game Score: 0.687

(h) Iteration 10, Episode 30, Defense Game Score: 0.912

Defense experimentalist + model calibrator

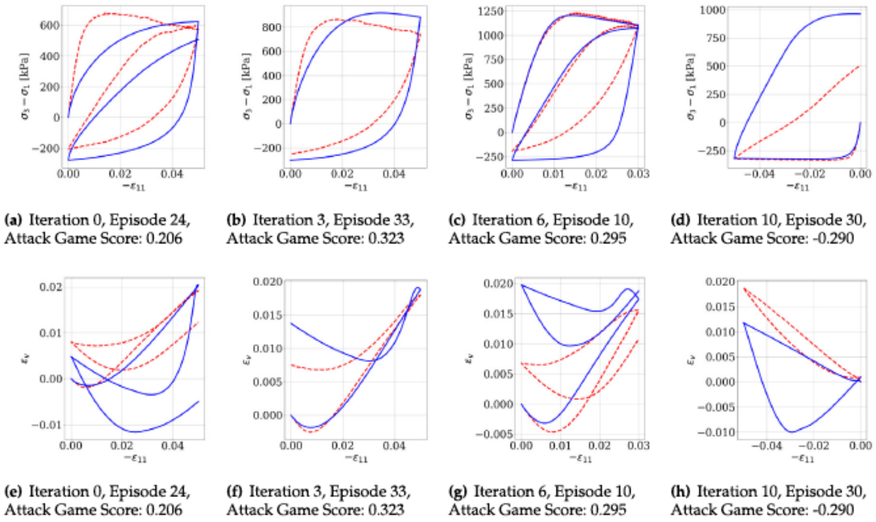

(a) Iteration 0, Episode 24, Attack Game Score: 0.206

(b) Iteration 3, Episode 33, Attack Game Score: 0.323

(c) Iteration 6, Episode 10, Attack Game Score: 0.295

(d) Iteration 10, Episode 30, Attack Game Score: -0.290

(e) Iteration 0, Episode 24, Attack Game Score: 0.206

(f) Iteration 3, Episode 33, Attack Game Score: 0.323

(g) Iteration 6, Episode 10, Attack Game Score: 0.295

(h) Iteration 10, Episode 30, Attack Game Score: -0.290

Attack experimentalist

Reinforcement learning performance of the experimentalist/adversary game (ML Traction- separation model)

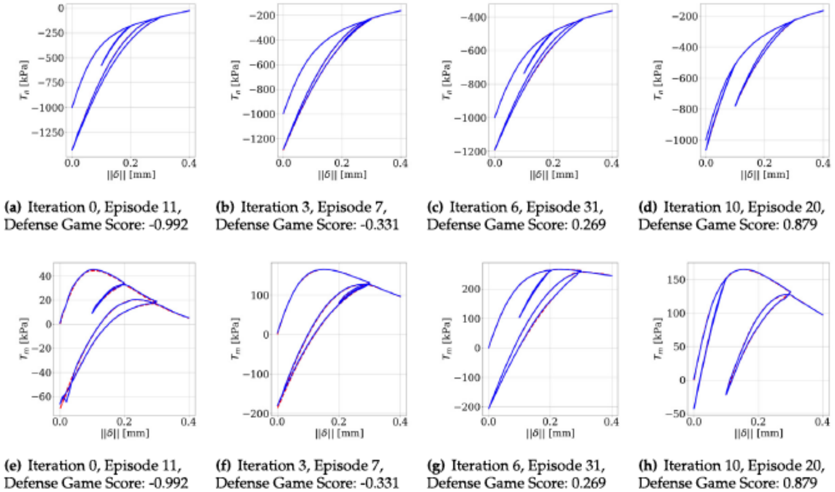

(a) Iteration 0, Episode 11, Defense Game Score: -0.992
(b) Iteration 3, Episode 7, Defense Game Score: -0.331
(c) Iteration 6, Episode 31, Defense Game Score: 0.269
(d) Iteration 10, Episode 20, Defense Game Score: 0.879

(e) Iteration 0, Episode 11, Defense Game Score: -0.992
(f) Iteration 3, Episode 7, Defense Game Score: -0.331
(g) Iteration 6, Episode 31, Defense Game Score: 0.269
(h) Iteration 10, Episode 20, Defense Game Score: 0.879

Defense experimentalist + model calibrator

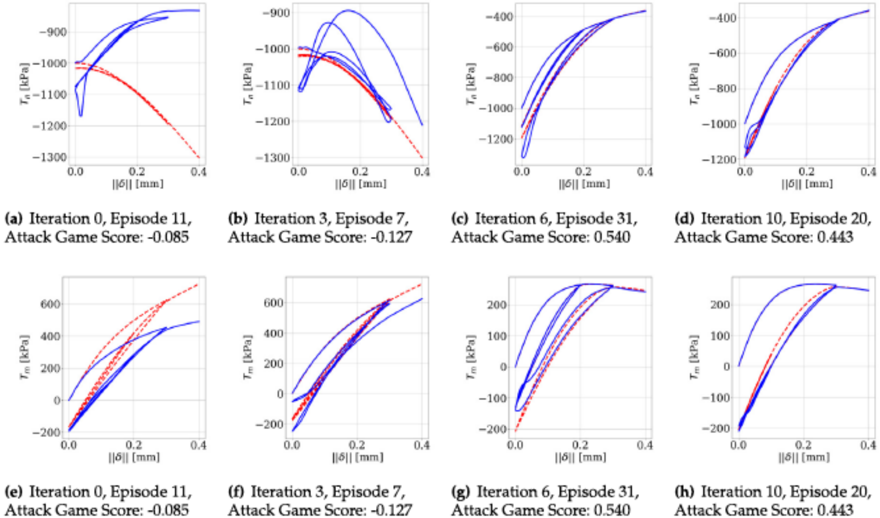

(a) Iteration 0, Episode 11, Attack Game Score: -0.085
(b) Iteration 3, Episode 7, Attack Game Score: -0.127
(c) Iteration 6, Episode 31, Attack Game Score: 0.540
(d) Iteration 10, Episode 20, Attack Game Score: 0.443

(e) Iteration 0, Episode 11, Attack Game Score: -0.085
(f) Iteration 3, Episode 7, Attack Game Score: -0.127
(g) Iteration 6, Episode 31, Attack Game Score: 0.540
(h) Iteration 10, Episode 20, Attack Game Score: 0.443

Attack experimentalist

Evolution of the estimated policy value

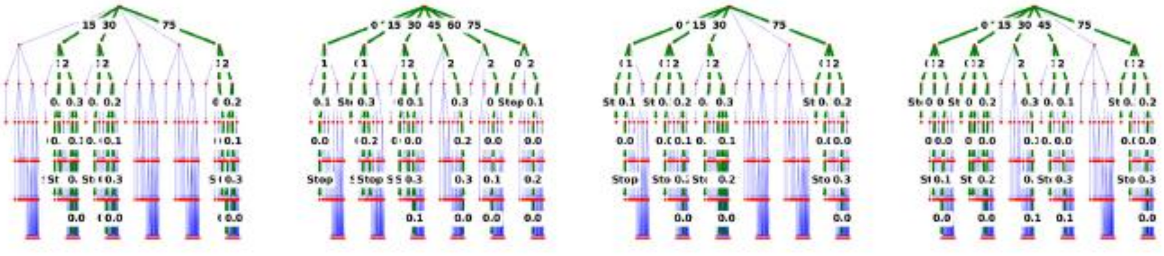

(a) Iteration 0, Episode 11, Defense Game Score: -0.992

(b) Iteration 3, Episode 7, Defense Game Score: -0.331

(c) Iteration 6, Episode 31, Defense Game Score: 0.269

(d) Iteration 10, Episode 20, Defense Game Score: 0.879

Fig. 21. Examples of paths (experiments) in the decision trees selected by the protagonist during the DRL training iterations for the traction–separation model.

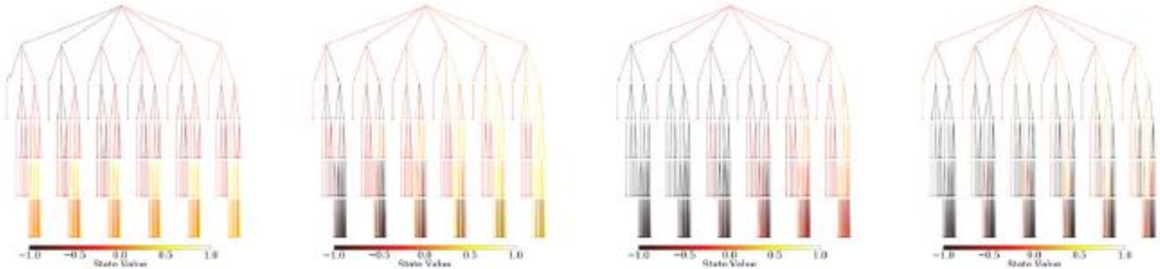

(a) Iteration 0

(b) Iteration 3

(c) Iteration 6

(d) Iteration 10

Fig. 22. Examples of Q-values of all possible states in the experimental decision tree estimated by the protagonist's policy/value network f_θ during the DRL training iterations for the traction–separation model.

Concluding Remarks:

1. This work focuses on two aspects of ML plasticity modeling, i.e. smoothness and interpretability.

2. The goal is to not to replace expert knowledge with black-box modeling but to create interface to create more accurate and precise model.

3. Extension is focusing on incorporate geometric learning to analyze evolution of microstructures.

4. What makes the model interpretable is not necessary only having the expression of equations but have the geometrical interpretation.

5. How to formulate the learning problems has a great impact on the quality of the predictions.

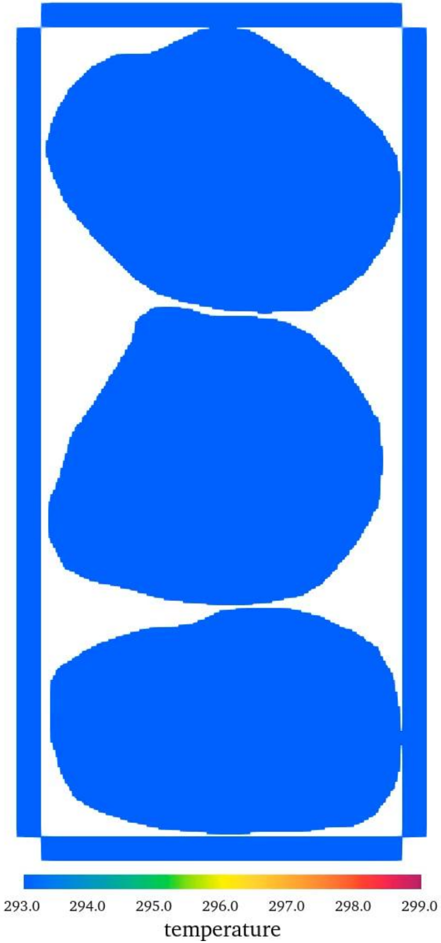

Acknowledgements

- Army Research Office: Young Investigator Program Award
- Air Force Office of Scientific Research, Young Investigator Program Award
- National Science Foundation: EAR-1516300 and CMMI-1445033, NSF CAREER
- Sandia National Laboratories
- US Department of Energy Office of Nuclear Energy
- Columbia University

Thank You!

More information can be found at
www.poromehanics.org